Dynamic Analysis of Flexible Turbo-Rotor System Using Super-Elements

by

A. Surial [1] and Dr. A. Kaushal [2]

[1] Rolls Royce, Montréal, Canada [2] Rolls Royce ,Montréal, and Ryerson Polytechnic University, Toronto, Canada

(514)631-6562

Abstract

The approach presented in this paper will give an overview on the dynamic analysis of gas turbine engines. It will help a user to prepare an input file for MSC/NASTRAN in order to perform the critical speed (SOL 107) and forced response analysis (unbalance response – SOL 108) of any size rotating structure(s), taking into account gyroscopic effects using MSC/NASTRAN DMAP, ridgyroa.v705.

1.0 Introduction

Over the past years, there has been a considerable research activity in the area of modeling and analysis of dynamic behavior of rotating structures. Some of the dynamic characteristics of interest are critical speeds, system stability and response to unbalanced excitation. In the design and retrofit process, it is frequently desirable and often necessary to adjust some system parameters in order to obtain a more favorable design or to meet the new operating requirements.

In the case of a gas turbine engine, the successful operation of the engine depends largely on the structural integrity of its rotating parts. The structural integrity in turn depends upon the ability to predict the dynamic behavior accurately and meet the design requirements to withstand steady and vibratory stresses. An accurate and reliable analysis of the rotor dynamic behavior is therefore essential and requires complex and sophisticated modeling of the engine spools rotating at different speeds, static structures like casings and frames and elastic connections simulating bearings.

Rotor dynamic analyses for a gas turbine engine model were carried out to determine critical speeds and the forced response due to unbalance . During the design stage the dynamic model is used to ensure that any potential harmful resonance's are outside the engine operating speed. Engine vibration tests are a part of the more comprehensive engine test program conducted on all development and production engines. All tests for the above engine were also conducted in the test cell at the Rolls-Royce Canada facility in Dorval to validate the analytical models.

2.0 Whole Engine Modeling

A finite element model of the whole Industrial Gas turbine engine has been developed and tested at Rolls Royce Canada Inc. Due to the complexity of the engine structure the model has been divided into four substructures modeled separately. The first substructure represents the engine casing, second - low pressure rotor (LP rotor), third - intermediate pressure rotor (IP rotor), and the fourth - high pressure rotor (HP rotor).

The engine casing (substructure 1) was modeled in MSC/NASTRAN using four-node quadrilateral (QUAD4) and three-node triangular (TRIA3) linear shell elements of the first order, and standard beam elements. The casing model is composed of eight modules representing the following components: a front inlet and low pressure compressor case (LPC case), intercompressor duct (ICD), plenum, aero intercase, combustor, low pressure turbine case (LPT case), rear mount structure, and a tail bearing housing (TBH). Such a division facilitates the implementation of any design changes to the engine casing. The casing model consists of about 8100 shell and 1000 beam elements, and about 50000 degrees of freedom. The finite

element mesh for the engine casing are shown in Figures 2.1 and 2.2.

The LP rotor model (substructure 2) was modeled in the Rolls-Royce finite element code - SC03 using about 3600 six-node triangular axisymmetric elements of the second order. The model has about 19000 degrees of freedom. This model was later reduced to 26 nodes located on the LP shaft center line using the Guyan reduction procedure together with the Fourier analysis. Such a reduced LP rotor model was transferred to MSC/NASTRAN to be connected with the engine casing model. Each node on the center line has six degrees of freedom, which represents the movement of the whole shaft in space. The stiffness and mass properties of the model exist in a matrix form and are associated with the center-line nodes of the LP shaft. Figure 2.3 shows the unreduced LP rotor model with Guyan nodes.

The IP rotor model (substructure 3) was modeled in the same way as the LP rotor model. The model consists of about 3000 six-node quadratic triangular axisymmetric elements, and about 16000 degrees of freedom. The reduced IP rotor model has 23 nodes located on the IP shaft centerline. The unreduced IP rotor model is presented in Figure 2.4

The HP rotor model (substructure 4), modeled similarly as the LP and IP rotors, comprises about 3050 six-node quadratic triangular elements, and about 15600 degrees of freedom. The reduced HP rotor model has 18 nodes located on the HP shaft centerline. The unreduced HP rotor model is presented in Figure 2.5.

These four substructures were combined together to set up the dynamic model for the whole engine. Figure 2.6 shows interface nodes between the casing and the rotors, and additionally, the location of the engine mounts.

3. Engine Dynamics

3.1. Dynamic Model – Critical Speeds

An MSC/NASTRAN dynamic model for the two-plane mount engine was constructed using the engine substructure models and the eight casing modules described in section 2. The model composed of the unreduced casing (substructure 1), and the reduced rotor models (substructures 2, 3 and 4). The different substructures were represented by superelements [1]. The half weight of the power train shaft was added to the corresponding interface node on the LP shaft centerline. The engine mounts were represented by equivalent stiffness springs.

Using the complex eigenvalue solution (SOL 107), the speed dependent gyroscopic terms were included in the system equations by utilizing MSC/NASTRAN ssalter ridgyroa.v705. This alter adds gyroscopic terms to dynamic analysis using the structured solution sequences. The alter supports either nonsynchronous or synchronous addition of the gyroscopic terms. In this analysis the nonsynchronous option is utilized which adds the gyroscopic terms that are proportional to the supplied speed of the LP rotor (3600-rpm). The gyroscopic terms for the IP

and the HP rotor speeds are calculated and scaled proportionally by utilizing the speed ratio between the rotors.

The complex Lanczos method was used to predict the critical speeds and mode shapes of the whole engine model. A combination of dynamic reduction and Lanczos method of complex eigenvalue solution was found to be more economical.

As expected, two critical speeds were obtained at each frequency, one corresponding to forward whirl and the other to reverse whirl. [2]. The whirl direction for the rotor (forward or backward) can be determined by animating the results in MSC/PATRAN. The critical speeds are shown in Table 3.1.

Three representative mode shapes for the LP rotor are presented in Figures 3.1 to 3.3. Similar plots were also produced for the IP and the HP rotor.

3.2. Dynamic Model – Forced Response

The dynamic engine model as described in section 3.1 was excited by an unbalance applied individually at LP compressor, LP turbine and shaft midpoint locations on the rotor. The frequency response was determined by sweeping through the range of interest at predetermined 1Hz intervals and at computed critical speeds. The frequency response was calculated for nonsynchronous condition including the gyroscopic effects. The response amplitudes in the X, Y and Z directions were obtained for several grid locations corresponding to different locations in the model, i.e. different LP grid locations (Figures 3.4 and 3.5). The structural damping was taken to be 10%.

4. Discussion Of Results

The model for calculating the critical speed analysis is described in Section 3.1.

There are 3 significant LP rotor modes close to the engine operating speed. (Table 3.1) The mode shapes for the LP rotor are shown in Figs. 3.1 to 3.3. The author's are in the process of calculating the strain energy content in the LP shaft associated with these modes to comply with the generally acceptable Rolls-Royce design standard. Animating the results in MSC/PATRAN can identify the whirl direction for the various modes. For the modes where the LPT shaft is in backward whirl, while the front of the LP rotor is in forward whirl, it is not known in what forms, if at all, these modes can appear in reality. The greatest orbits for these modes occur at the LPT area.

Figure 3.4 shows the LP rotor forced response in the Y direction at the LP compressor disk position. A major peak can be seen at about 37 Hz with the greatest amplitude of approximately, 0.0037".

Figure 3.5 presents the LP rotor unbalance response at the first LP turbine disk position for

the same model. A major peak can be identified at about 46 Hz with a maximum amplitude level of about 0.0031".

All the peaks shown in the forced response plots can be associated with the predicted critical speeds for this engine model.

Similar analysis was also carried out for the IP and the HP excited critical speeds.

4.2. Conclusions

The method in this paper allows the MSC/NASTRAN user to perform the critical speed (SOL 107) and forced response analysis (unbalance response – SOL 108) of any size rotating structure(s), taking into account gyroscopic effects using MSC/NASTRAN DMAP, ridgyroa.v705.

The paper has examined only a few of the possible methods of representing the gyroscopic effect in MSC/NASTRAN dynamic solutions. The procedure implemented in MSC/NASTRAN allows the rotating structure(s) to be modeled using Rolls Royce SC03, utilizing axi-symmetric capability, to reduce the model size. The rotating model(s) are attached to the static structure using the super-elements approach.

This procedure has been implement and produced reasonable results for the Industrial Trent engine.

4.3. Acknowledgments

The authors are grateful to the management at Rolls Royce Canada, especially Ed Green and John Uings, for allowing them to use the library and receive assistance in putting this document together, The authors would also like to thank the members of the selection committee at MSC, for giving them an opportunity to share their views and experience in this technology area.

4.4. References

[1] "MSC/Nastran - Handbook for Superelement Analysis", The MacNeal-Schwendler Corp., Los Angeles.

[2] "Mechanical Vibrations", Den Hartog, J.P., 4th ed. Mcgraw Hill, New York.

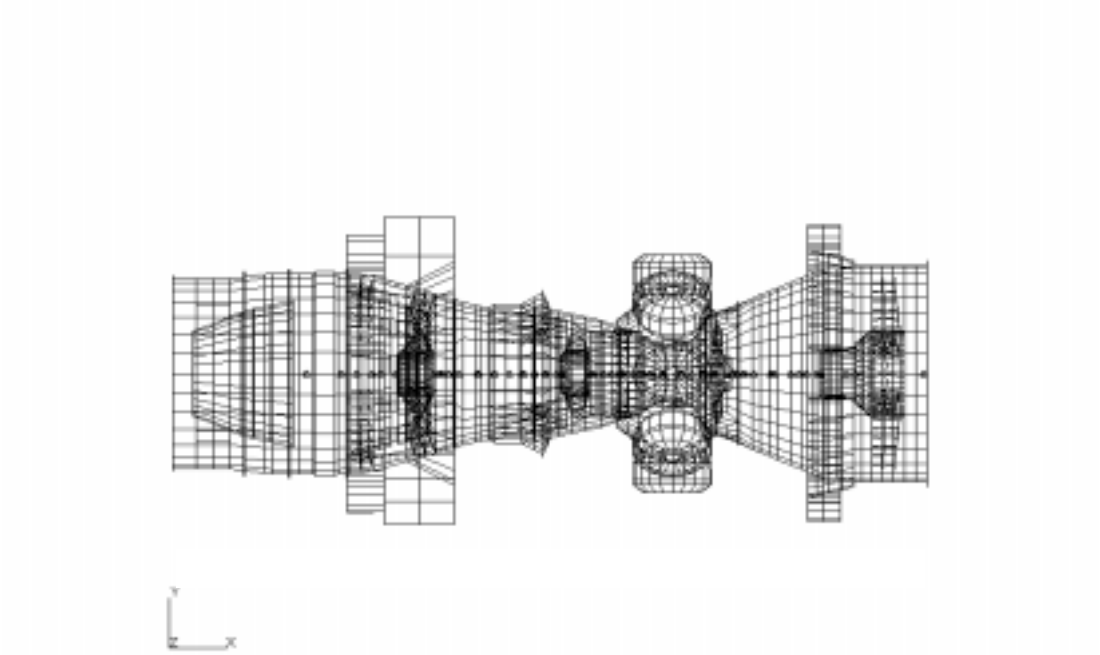

Figure 2 .1 : Finite Element Model – Engine Casing (Side View)

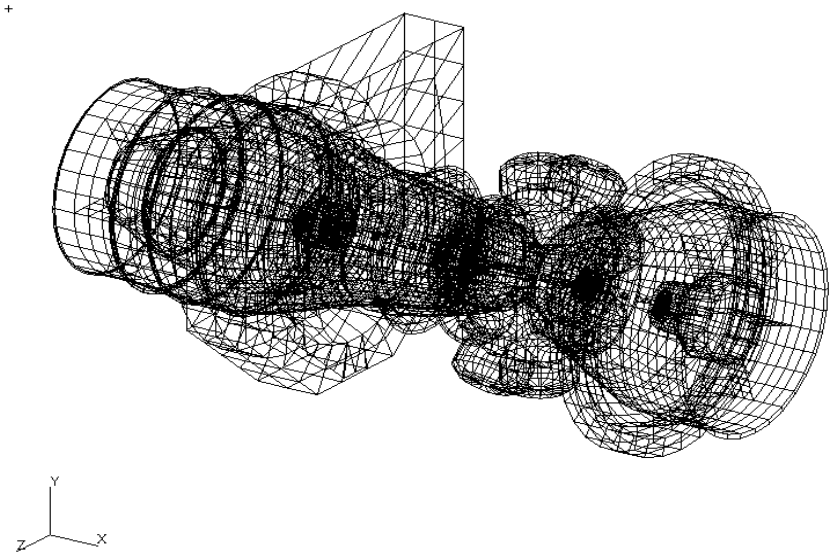

Figure 2. 2 : Finite Element Model – Engine Casing (Isometric View)

Figure 2 .3 : LP Rotor Guyan Points

Figure 2 .4 : IP Rotor Guyan Points

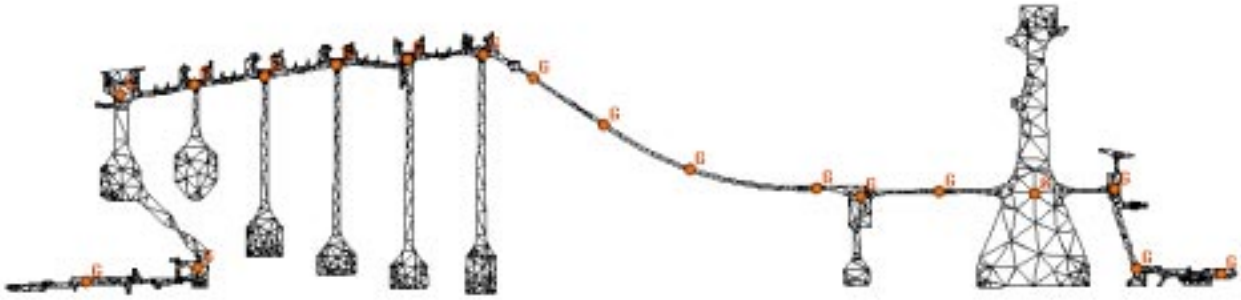

Figure 2 .5 : HP Rotor Guyan Points

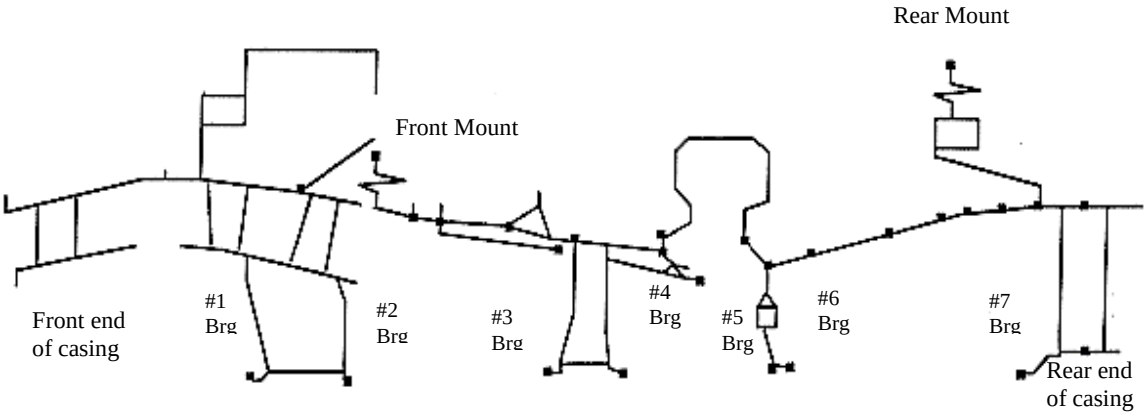

Figure 2.6 : Casing-Rotor Interfaces and Engine Mounts

Table 3.1 : Critical Speeds

Mode #	Freq. (Hz)
2	3.58
3	4.77
4	5.08
5	8.11
6	8.59
10	14.45
11	16.00
15	22.73
20	36.7
21	41.56
22	44.31
23	45.20
24	48.34
25	52.55
26	54.51
27	57.42
28	61.43
29	62.55
30	63.04
31	70.39

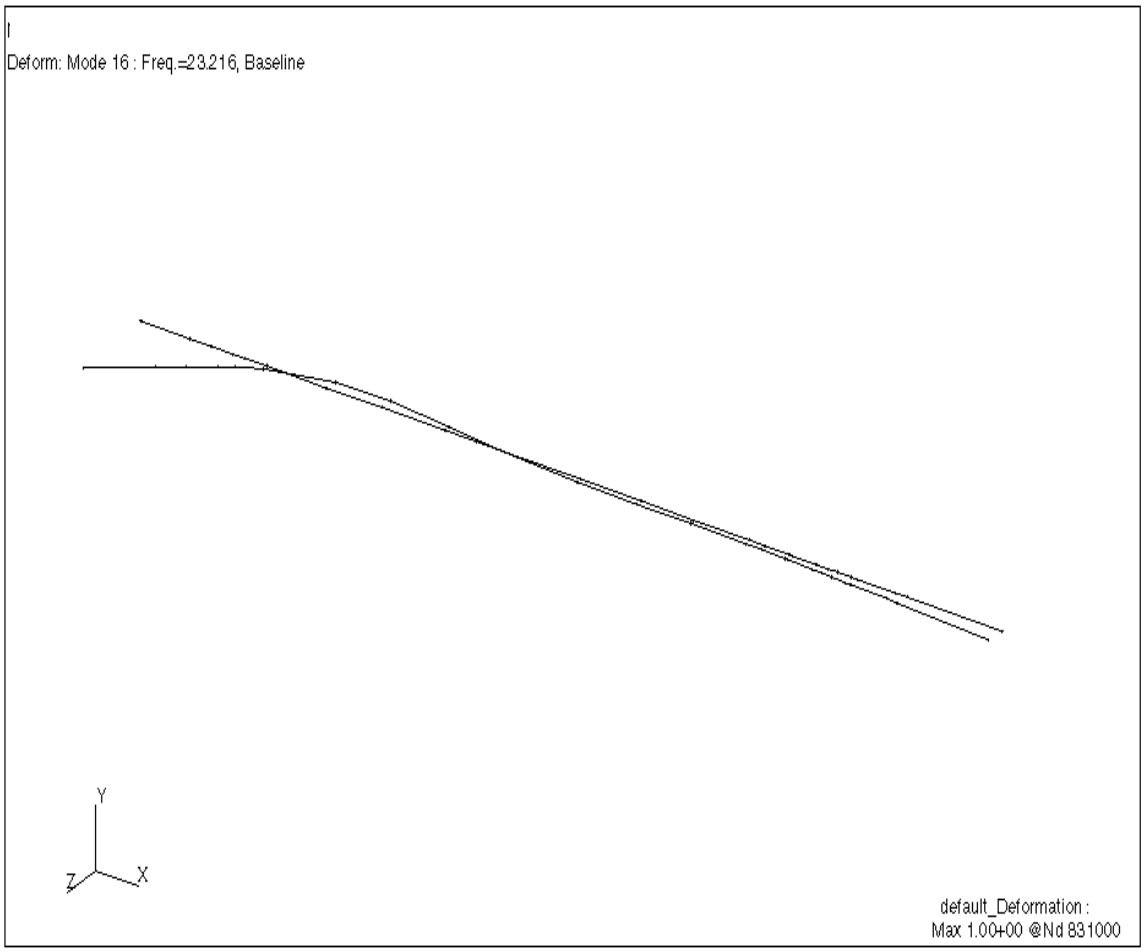

Figure 3.1 : LP Excited Critical Speed – 23.12 Hz

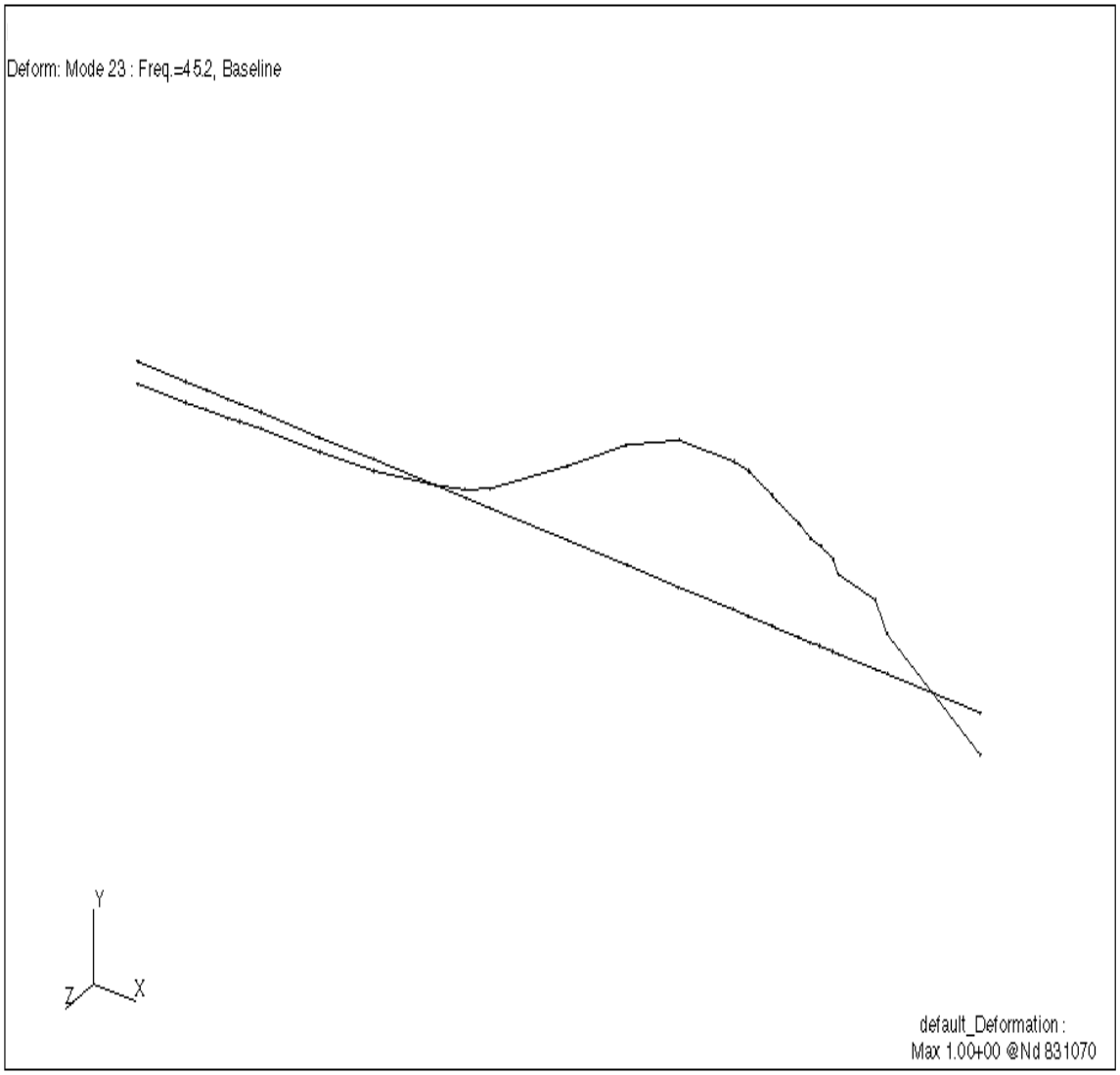

Figure 3.2 : LP Excited Critical Speed – 45.2 Hz

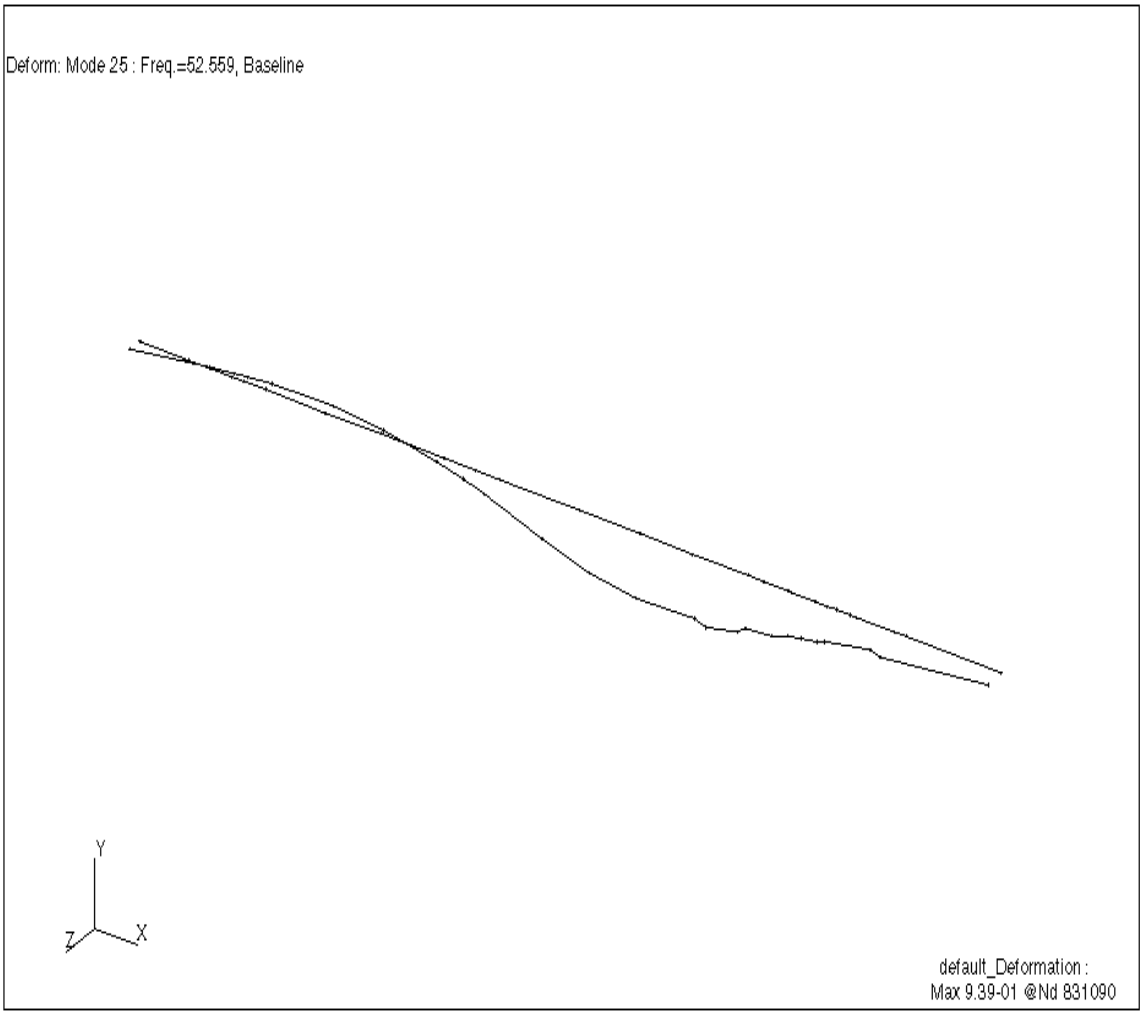

Figure 3.3 : LP Excited Critical Speed – 52.55 Hz

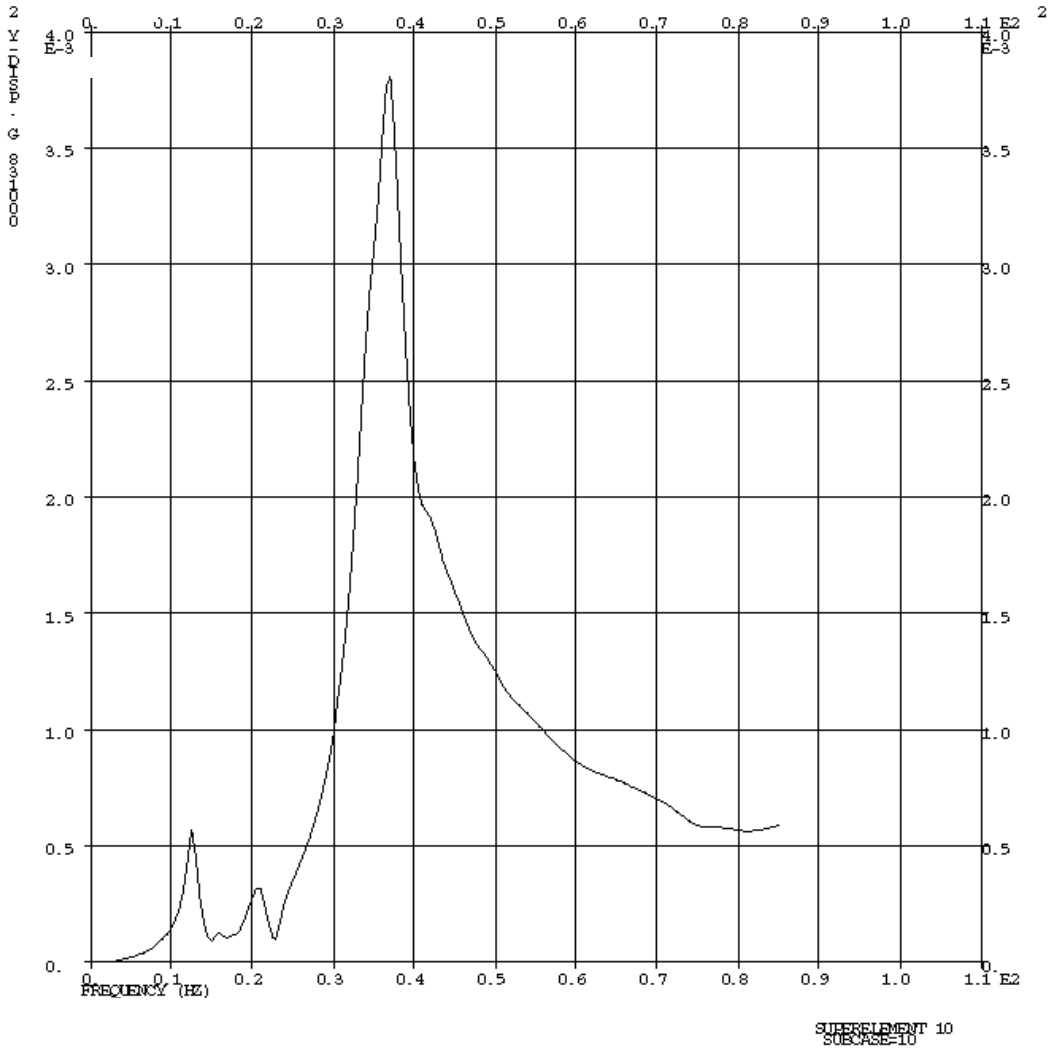

Figure 3.4 : Out of Balance Response – LPC Grid

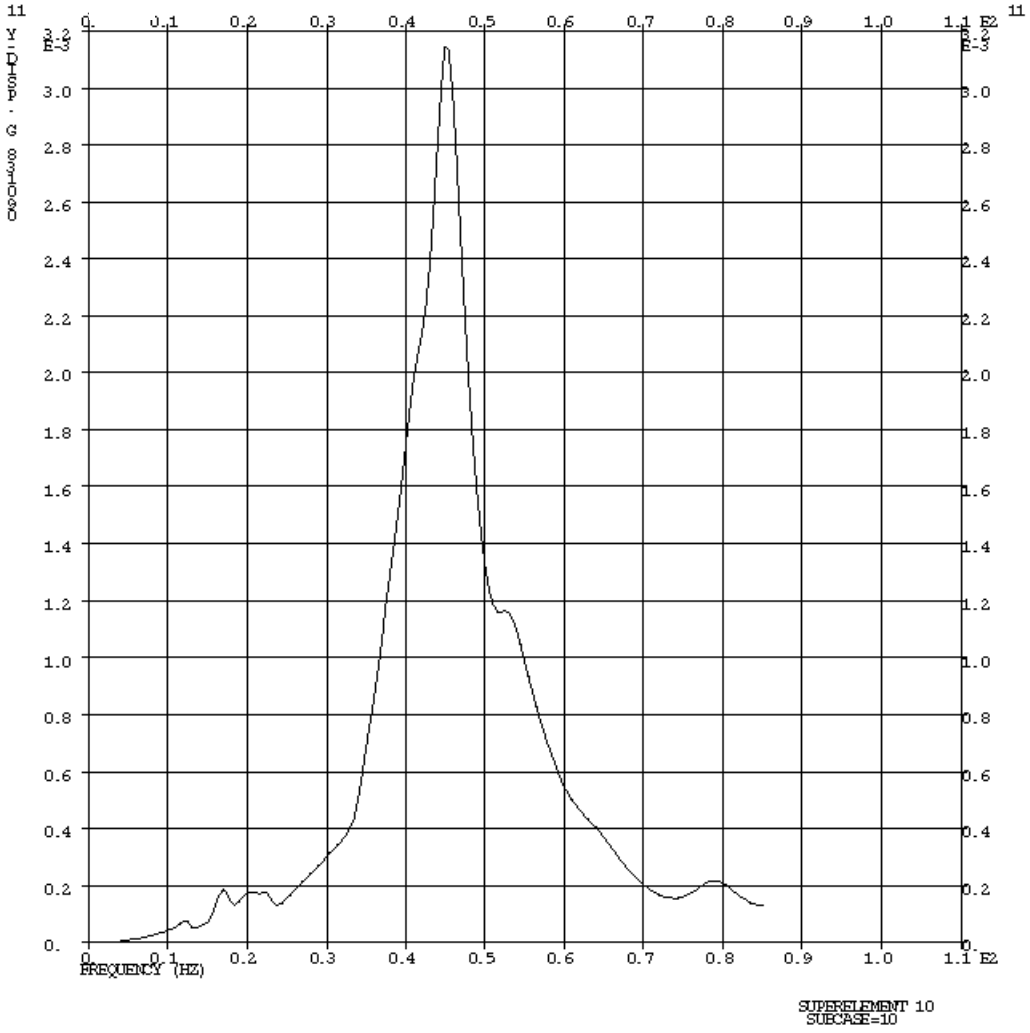

Figure 3.5 : Out of Balance Response – LPT Grid